GeoVirtual 2020 September 14-16
Resilience and Innovation

Effect of spatial variability of foliation orientation on mining slope design

Joseph Kabuya Mukendi, Richard Simon
Dept. of Civil, Geological and Mining Engineering – Polytechnique Montréal, Montréal, Québec, Canada

ABSTRACT
Local variation in the foliated nature of the rock mass can have a significant effect on mining slope design, and it is often difficult to predict. This issue should be considered in pit design and continuously monitored during mine development. This paper describes the huge challenge of building the final southeastern wall of the Z pit pushback by mitigating the risk of slope failure caused by the spatial variability of the foliation orientation, knowing that previous mining in this sector of the pit had caused a multi-bench failure 125 m high and 200 m wide. The methodology based mainly on bench face cleanup, design compliance analysis, televiewer surveys, the modification of the blasting techniques and radar monitoring, made it possible to achieve optimal slope and to continue mining safely.

RÉSUMÉ
La variation locale de la nature foliée de la masse rocheuse peut avoir un effet significatif sur la conception des pentes minières et elle est souvent difficile à prévoir. Cela constitue une préoccupation qui devrait être prise en compte pour la conception d'une fosse et qui devrait être surveillée en continu pendant le développement de la mine. Cet article décrit l'énorme défi qui consistait à construire le mur sud-est final de la fosse Z en atténuant le risque de rupture de pente causée par la variabilité spatiale de l'orientation de la foliation, sachant que l'exploitation minière antérieure dans ce secteur de la fosse avait causé une rupture de pente de 125 m de haut et 200 m de large. La méthodologie basée principalement sur le nettoyage de la face de pente, l'analyse de conformité de la conception, les relevés géophysiques, la modification des techniques de dynamitage et la surveillance au moyen du radar a permis de construire une pente optimale et de poursuivre l'exploitation en toute sécurité.

1 INTRODUCTION

The design of open pit mining slopes uses a structural model that describes the orientation and spatial distribution of the geological structures and the subdivision of the rock mass into structural domains. These structural domains are differentiated by the presence of faults, changes in lithology and alteration profiles, as well as changes in the orientation of geological structures such as the foliation. Foliation is due to viscous flow, crystal growth at high pressures and temperatures and shearing under high confining pressure over geological era (Read and Stacey, 2009). This means that local orientations of the foliation are often difficult to predict and can have a significant effect on slope design. This issue should be considered in pit design and continuously monitored during mine development.

This paper describes the huge challenge of building the southeastern final wall of the Z pit pushback (Figure 1) by mitigating the risk of slope failure caused by spatial variability of the foliation orientation, knowing that previous mining in this sector of the pit had caused a multi-bench failure 125 m high and 200 m wide.

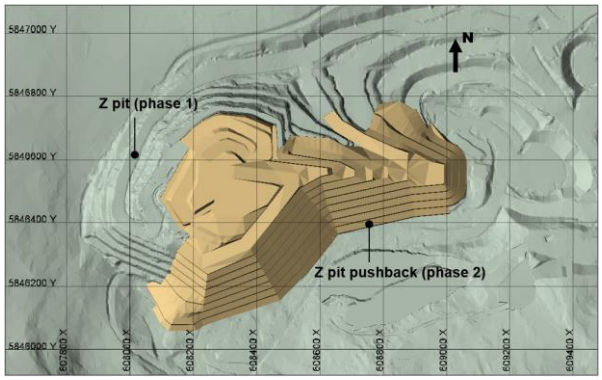

Figure 1. Z pit phases 1 and 2 (pushback)

Z pit is a metal mine in eastern Canada.The foliation is the most prominent structure at the mine site and it is observed to be one of the controlling factors with respect to pit wall design and stability. The results of

this study are expected to be informative for the other pits in the mining site where similar geotechnical conditions exist.

2 PREVIOUS HIGHWALL FAILURE

The structural geology in the mine site area studied is complex due to tight folding caused by at least two major orogeny events. The end result of the complex folding at the Z pit was the creation of a tight fold with limbs generally dipping southeast. The quartzite (QR) which forms the main lithology of the southeast wall is usually a hard, white, massive rock with variable amounts of muscovite, low amounts of garnet and biotite, and variable hematite content as it approaches the upper contact with the iron formation (IF) (Piteau, 2016).

A highwall failure occurred in the southeast region of the Z pit (phase 1). The highwall instability was detected by slope stability radar and resulted in a multi-bench failure containing an estimated 3,000,000 tonnes of rock, becoming one of the most significant instability events to have occurred at the mine site (see Figure 2 for post-failure photograph). The unstable highwall was over 125 m high and 200 m wide. The overall slope angle before failure was 44°. The failure area consisted mainly of a mass of foliated QR, limited by contact with a more competent IF that was exposed on the pit wall. The radar monitoring system was thus considered to be effective for its purpose, having provided sufficient warning of the imminent collapse to allow for evacuation of personnel and equipment from the area.

Figure 2. Southeast highwall post-failure photograph

Kabuya et al. (2020a) completed a numerical modelling study to back-analyse this highwall instability event which occurred in the Z pit. An attempt has been made to calibrate simplified models developed in SLIDE3 and RS2 to reproduce this highwall instability. One of the purposes was to develop an understanding of the mechanisms and key parameters sensitivities, with regard to stability, which may have been involved in the highwall failure. Figure 3 presents the stereonet representation of the discontinuity sets and orientations in the immediate area of the highwall instability. Structural interpretation indicated that the dip of discontinuities along the foliation may flatten and become progressively shallower with increasing pit depth. Separate structural regimes were defined for the upper and lower slopes in the failure area. A horizontal dividing plane was defined approximately 70 m below the crest of the pit slope, with steeply dipping foliation (FL-1B) above and more shallowly dipping foliation (FL-1C) below. This model was considered the best estimate of the structural features of the highwall failure (elevation-dependent foliation).

Through experimentation, it was found that reproducing the instability of the highwall was critically sensitive to the local structural characterisation. The modelled solution was to significantly weaken the sub-horizontal BD-1 joint set to produce a factor of safety (or critical strength reduction factor) approaching the target of 1.0 and to initiate toe breakout. The local orientation of QR foliation may continue to rotate (fold) with depth, to provide the necessary toe weakness in place of a weakened BD-1 set, but this local variation would not be captured in a domain-scale structural characterisation.

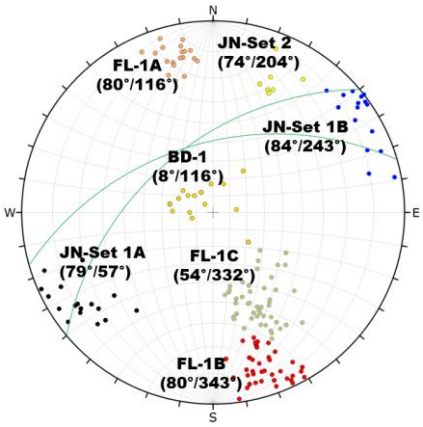

Figure 3. Structural interpretations of the southeast region of the Z pit (Kabuya and Henriquez, 2017)

3 BACKGROUND

In 2019, slope failures were observed on the pushback wall in the southeast region of the Z pit. Crest losses between levels 700 and 728 occurred in the QR. It can be observed (Figure 4 and Figure 5) that failure materials accumulated at the toe of the slope and the presence of slabs on the bench face. These losses in catch-bench width seemed to follow the same plane, with variable orientation. The presence of a fault was suspected since the orientation of this plane is similar to that which caused the highwall failure located in front of the current slope (phase 1). The height of the overall slope is 84 m and is expected to reach 252 m.

In order to continue mining safely, this study was initiated as part of a risk management plan. The methodology was mainly based on the bench cleanup, the design compliance analysis, the televiewer surveys, the modification of blasting techniques and the radar monitoring. This is discussed in the next sections.

Figure 4. Slope failure and slabs observed on the southeast wall (bench 700-728)

Figure 5. Slope failure and slabs observed on the southeast wall (bench 700-728)

4 BENCH FACE CLEANUP

The wall of the southeast region resulted in a foliation plan undercut and the slabs remained on the bench face. The slabs remaining on the bench face created a potential safety hazard that should be removed. Secondary scaling of bench faces was performed with the equipment positioned on the bench floor. Scaling from the bench above by chaining the face using a chain with attached dozer track plates was not possible due to the reduced bench width remaining. To eliminate all slabs remaining at the crest, it was decided to blast the slabs along the plan of foliation where it was possible. Figure 6 shows the bench face cleanup and the post-blast materials accumulated at the toe of the bench, which would also be cleaned up.

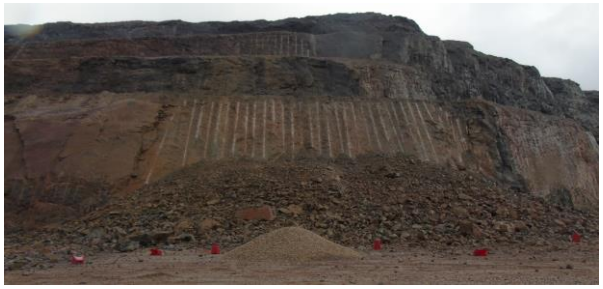

Figure 6. Bench face cleanup

5 SLOPE PERFORMANCE ASSESSMENT

The assessment of the performance of the benches is an important component of any slope assessment program. The factors influencing slope performance are complex and cannot all be explicitly taken into account. The comparison of the as-built bench face angles with the expected bench face angles and the as-built bench widths versus the as-designed bench widths are an opportunity for objectively assessing the performance of the slope. Although these comparisons make it possible to assess whether the implementation of the design has been respected according to the established criteria, the evaluation of the performance of the slope should also evaluate the effectiveness of the design (Read and Stacey, 2009).

The design criteria for the pushback in the southeast region of the pit were determined in an earlier study (Henriquez et al., 2018). It was recommended to develop a benched presplit slope with bench faces mined at 70°, a bench height of 28 m and berm width of 14 m. In order to assess the performance of the benches, the comparison of the as-built benches and the designed benches was conducted from a photogrammetric survey on the exposed wall. This made it possible to quantify the breakback and the final wall slope angle. PerfectDig software (Maptek, 2018) was used for this purpose. Figure 7 shows the overbreak area along the benches. A total of 10,208 tonnes represents the overbreak tonnages. Figure 8 represents the as-built bench face versus the designed bench face along the section A-A.

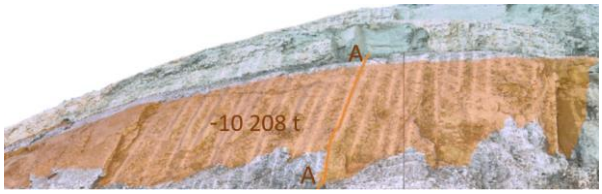

Figure 7. Overbreak area along benches

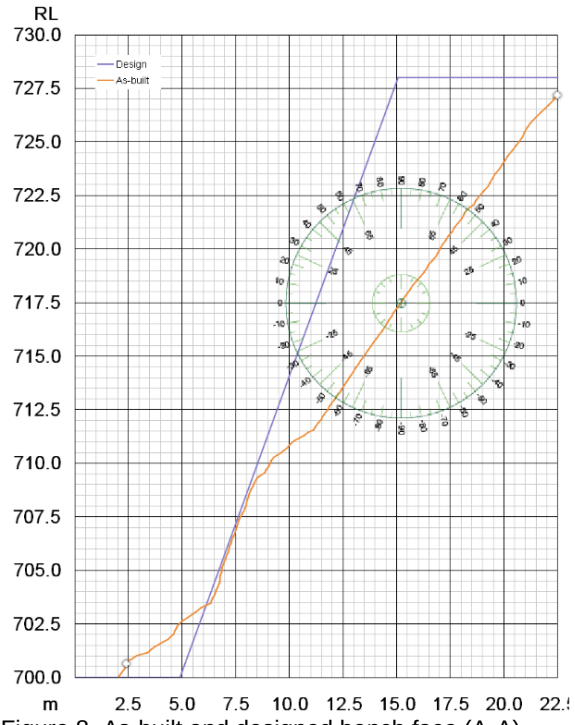

Figure 8. As-built and designed bench face (A-A)

It can be observed that the breakback is almost 8 m. The overbreak zone of the pit wall is observed from the crest to the 709.5 m level. The as-built slope face angle is 55°. Conformity to design is observed from 709.5 m to 703 m. This indicates that the presplit was made at 70°, according to the design, and undercut the foliation, causing the slope failures observed. Loose materials are observed between 703.5 and 700 m. Cleanup of loose materials along the bench toe would be required to continue mining operations.

6 TELEVIEWER SURVEYS

6.1 Objectives

The major difference observed between the designed bench and the as-built bench was due to the local orientations of discontinuity set, which had not been detected at the time of the slope design. The structural geology surveys were then required in order to continue mining safely.

Geophysical surveys were conducted in a series of eight boreholes identified as TV19-01 to TV19-08, all located near the Z pit's southeast wall. The boreholes are all PQ size with a 70° inclination and 160° azimuth (Figure 9).

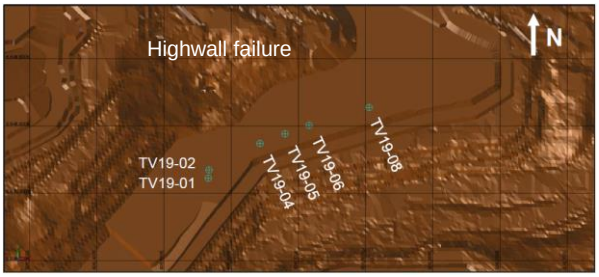

Figure 9. Locations of televiewer holes

The purpose of the surveys was to detect and orient the structures intersected by boreholes. The investigation program consisted of an optical and acoustic televiewer survey of borehole walls and a profile survey of borehole diameter variations using a caliper probe. The optical televiewer survey was conducted from the surface to the bottom of all boreholes. The acoustic televiewer survey was conducted in the submerged portion of the boreholes. Note that the quality of the optical televiewer image in the submerged portion of the boreholes was affected by the opacity of the water found in them. The surveys in holes TV19-03 and TV19-07 were not completed as the survey equipment got stuck at 3 m and 2 m, respectively. A total of approximately 502 m of logs were collected in the boreholes from the surface.

6.2 Data acquisition

The data was collected with a Matrix digital logging system and an MXC-1000 winch. The system measures depth using a high-resolution optical encoder. The data is recorded on a laptop computer and displayed in real time, making it possible to assess data quality during the survey.

Caliper log: Caliper data was collected with a 2CAA-1000 mechanical probe. The caliper provides direct data of the average borehole diameter along its axis. The diameter is determined by the extension of three spring-loaded arms that slide along borehole walls. Caliper logs were recorded from the bottom of the borehole upwards using a sampling interval of 10 mm and a probe ascent rate of 2.5 to 4 m/min.

Optical televiewer (OTV) logs: The OBI40 optical borehole imager was used to generate high-resolution digital images of the inside of borehole walls. OTV logs were recorded from the top of the borehole downwards using a downward speed of 1 to 1.5 m/min, a sampling interval of 1.7 mm and an azimuthal resolution of 1°.

Acoustic televiewer (ATV) logs: The acoustic camera data was taken with an ABI40 probe. ATV logs were recorded from the bottom of the borehole upwards using a sampling interval of 2.1 mm and a probe upward speed of 1.5 to 2 m/min. The acoustic camera was deployed in the water-filled portion of the boreholes to produce an image of the borehole wall based on the amplitude and travel time of the acoustic waves reflected from the rock formation wall (Golder, 2019).

Figure 10 shows televiewer surveys of borehole TV19-08. The tripod and the cable supporting the probe in the borehole are visible. The depths of the logs completed on-site are shown in Table 1. They vary from 26.91 m to 28.90 m.


Figure 10. Televiewer surveys of the TV19-08 hole

Table 1. Characteristics of televiewer holes

Holes	Caliper (m)	Optical (m)	Acoustic (m)
TV19-01	28.12	27.43	27.47
TV19-02	28.49	27.57	27.93
TV19-04	27.97	26.94	27.99
TV19-05	28.90	27.46	28.50
TV19-06	28.62	26.91	28.61
TV19-08	28.87	27.18	27.47

The images taken by the optical and acoustic cameras are oriented by simultaneously recording data from a three-axis fluxgate magnetometer and three accelerometers built into the probes. Prior to interpretation, the image is oriented to a global reference, either magnetic north or the top of the borehole. Generally, images are oriented to magnetic north in boreholes with an inclination greater than 80 degrees relative to the horizontal plane. For boreholes with an inclination of less than 80 degrees, the image is first oriented with the top of the borehole before being oriented to magnetic north.

The planes of the structures intersecting the borehole wall produce sinusoidal traces in the camera image. Using the reference direction recorded during the logging, the sinusoidal traces are analyzed to obtain the dip and direction of the structures (Golder, 2019).

6.3 Data analysis

The steps for processing log data are as follows:

- Raw data is imported into WellCAD (RocWare, 2016), a software designed to manipulate and present log data;
- Corrections are then applied to the different logs (caliper, optical and acoustic cameras) to account for the height of the drill collar and make all depths consistent from the ground surface. As part of this procedure, a verification is also conducted to ensure that the characteristics common to the different logs (for example, a large structure) are recorded at the same depth;
- The structures observed in the optical and acoustic camera images are interpreted and oriented towards magnetic north. The dip is calculated in relation to the horizontal plane; and,
- The logs of all probes used in boreholes are presented together in a single figure for analysis and interpretation (Figures 11 to 16). The legend is presented in figure 17.

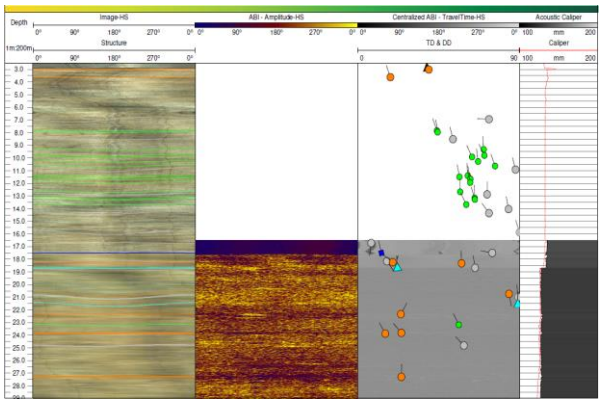

Figure 11. TV19-01 log

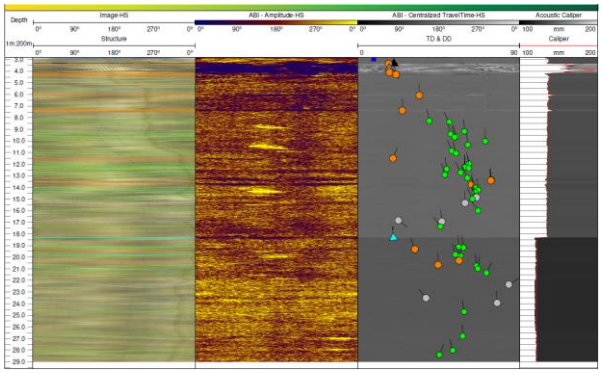

Figure 12. TV19-02 log

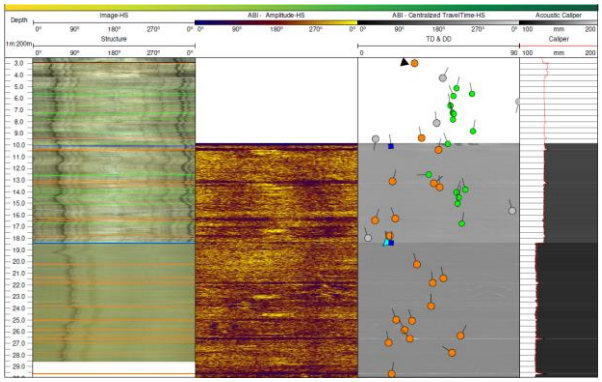

Figure 13. TV19-04 log

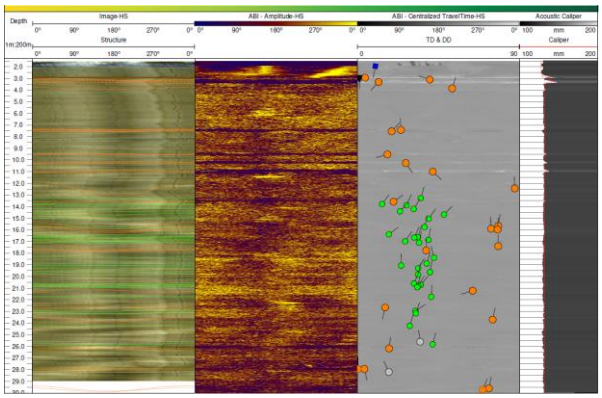

Figure 14. TV19-05 log

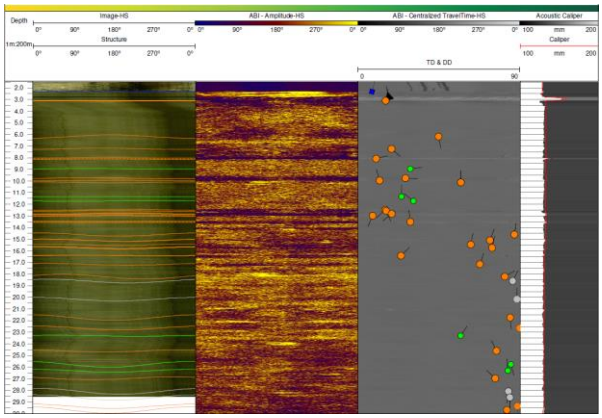

Figure 15. TV19-06 log

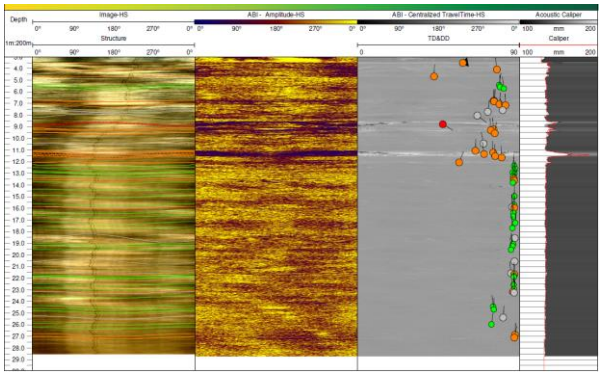

Figure 16. TV19-08 log

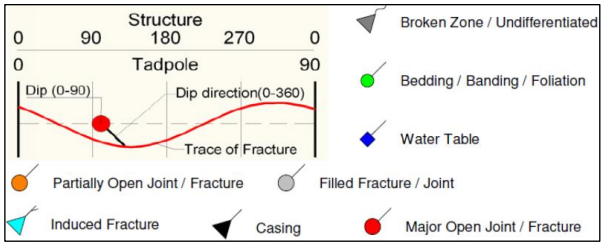

Figure 17. Legend of Figures 11 to 16

6.4 Results and interpretation

The results of the logs are presented in the form of stereonets (Figures 18 to 20). The Terzaghi correction was applied for the calculation of the concentration of the density of the poles illustrated in these figures.

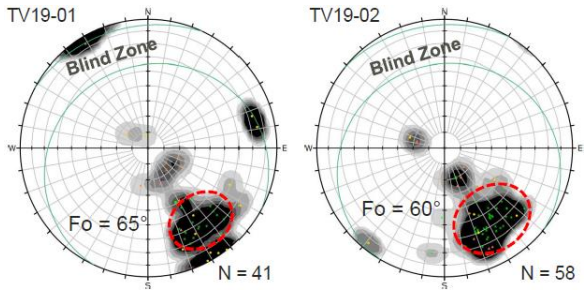

Figure 18. Stereonets of TV19-01 and TV19-02

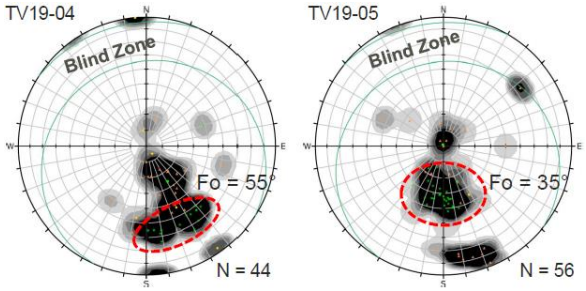

Figure 19. Stereonets of TV19-04 and TV19-05

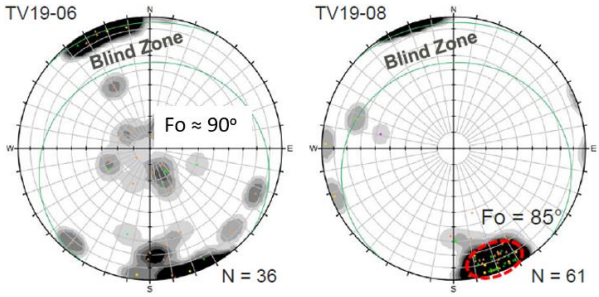

Figure 20. Stereonets of TV19-06 and TV19-08

The results of this investigation suggest that the plane on which the rupture occurred is not a fault but rather a plan of foliation associated with the bedding, which changes direction in this sector. It can be seen in the figures that it is a set of discontinuities whose orientation varies along the strike of the wall. For TV19-06 hole, the foliation dip seems subvertical although little data has been collected.

The southeast wall is currently being developed assuming that the bedding is facing the wall. The results of these televiewer surveys suggest that the bedding is rather oriented towards the pit and that this wall should be developed as a footwall following the foliation dip. Otherwise, the results suggest that a partially open QR/IF contact, parallel to the wall, is present only at the small eastern area. This was observed only in the TV19-8 hole at 11.4 m. The wall should be monitored during mining operations in the location of this hole.

7 CONTROLLED BLASTING

With increased understanding of foliation variability, improved blast designs were required. The southeast wall is currently being developed as a benched presplit slope with bench faces mined at 70°. As mentioned, the results of the televiewer surveys suggest that it should be developed as a footwall following the foliation dip and its variation along the strike. The foliation set may control design because it is closely spaced, continuous and planar. Furthermore, controlled blasting techniques must be applied to reduce blast-induced slope damage.

Trim blasting is the most commonly used controlled blasting technique because it can provide good results in a wide variety of geological conditions (Read and Stacey, 2009). Trim blasting parallel to foliation was recommended. Stabs rows are required to ensure that the rock breaks to the desired foliation dip and they are typically loaded to less than half of the hole height. A smaller diameter drill (254 mm) with tighter spacing will be used instead of a production drill (349.25 mm) to reduce both cratering and the chance of undercutting the foliation.

Usually, at the mine site, when mining footwalls, the bench face angle is based on measured orientation from the bench above. As foliation orientation is locally variable along the strike and depth, this practice presents the risk of undercutting the foliation. Trim blasting parallel to the foliation with a free face was therefore recommended. This provided an opportunity

to adjust the bench face angles based on measured foliation orientation along a free face at the same level as that to be mined. Figure 21 shows the free face between levels 686-700, on which the spatial variability of the foliation orientation along the strike has been determined from the photogrammetric survey and then used in the blast design.

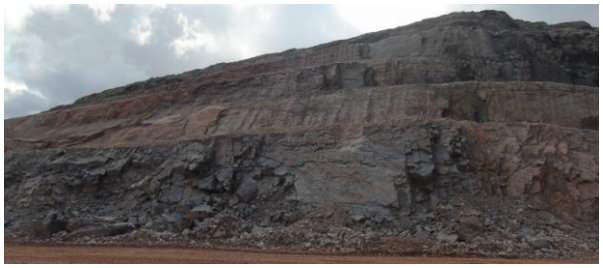

Figure 21. Free face between levels 686-700

Figure 22 shows the final wall built. It presents good blast performance compared to the bench above by reducing rockfall hazard through a cleaner bench face. Final wall design refinement is still ongoing at the mine site.

Figure 22. Final wall

8 RADAR MONITORING

To better manage the rockfall and slope failure risks, different systems for monitoring slope movements are used. Slope movement monitoring systems aim to minimize the impact of slope failure by predicting potentially unstable areas and provide geotechnical information to analyze the slope instability mechanism that develops (Read and Stacey, 2009). For large scale monitoring, Slope Stability Radar (SSR) can be used (Noon, 2003; Kabuya et al., 2020a). Radar, like all monitoring technology, has inherent physical limitations: instability less than 1.5 times pixel size may not be detected; areas covered by vegetation are generally not suitable for monitoring with radar; low coherence caused by vegetation, snow, water or loose rock material may result in unreliable results and data contamination; all slope stability radars are line-of-sight monitoring instruments; only the component of the displacement vector that is parallel to the radar signal will be measured; machinery interaction can cause data contamination, spikes in amplitude and low coherence; significant rainfall events can cause total loss of coherence over the scan area; coherence must remain high for a radar to be able to effectively measure displacement; the real aperture radar RAR (SSR-XT or FX) is not capable of monitoring movement once it reaches a velocity close to 8 mm per scan or faster; a synthetic aperture radar SARx is not capable of monitoring or tracking movement approaching a rate of 4 mm per scan or more (GroundProbe, 2020).

Figure 23 presents the SSR monitoring of the southeast wall. A project-specific trigger action response plan was developed. Alarm thresholds were set, and an intervention plan following radar alarms was implemented as part of controlling the slope instability risk. The current deformation rate of the slope is used as the reference velocity. It corresponds to the green alarm, indicating a normal continuation of mining operations. Any increase of 25% in velocity corresponds to the yellow alarm, resulting in increased geotechnical inspections and preparation for pit evacuation. Any increase of 50% corresponds to the orange alarm, resulting in the evacuation of the pit. Any increase of 75% corresponds to the red alarm, resulting in the pit being closed until the slope is stable again.

Figure 23. Slope Stability Radar monitoring the southeast wall

Figure 24 shows the radar image of the southeast wall. It can be seen that the deformation trend is still linear for the selected control points that are used for the long-term deformation analysis, and the wall is stable. The vertical steps in the deformation plot are residual errors due to atmospheric anomalies that occurred during short periods of time.

With the SSR, post-blast stabilisation time is measured following each blast. It corresponds to the time between the moment of blasting and the moment when the deformation rate becomes constant again. The resumption of mining activities in the pit after each blast can start safely after this post-blast stabilisation time. The degree of the blasting damage on the slope

can also be determined based on the time-to-stable period (Saunders et al., 2020; Kabuya et al., 2020b).

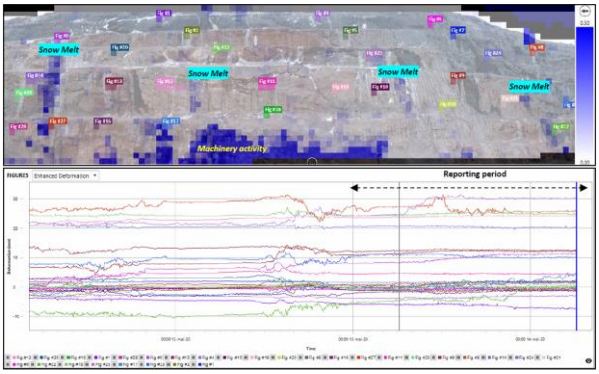

Figure 24. Radar image and deformation plot

9 CONCLUSION

Slope failures were observed on the pushback wall in the southeast region of the Z pit. The major difference observed between the designed and as-built bench was due to the local variability of the foliation orientation and led to structural geology surveys being performed in order to continue mining safely. The results of these televiewer surveys suggest that the bedding is not facing the wall as previously assumed but is oriented towards the pit, and that this wall should be developed as a footwall. This led to a change in the blasting techniques from systematic 70° pre-splitting to trim blasting parallel to foliation with a free face, for which the spatial variability of the foliation orientation can be determined from a photogrammetric survey to be used in the blasting design. This produces good blast performance compared to the bench above by reducing rockfall hazard through a cleaner bench face. To better manage the rockfall and slope failure risks, SSR monitoring is used. Alarm thresholds are set, and an intervention plan following radar alarms is implemented. After each blast, mining activities in the pit resume safely once the post-blast stabilisation time is observed and measured by the SSR.

This case study demonstrates that the spatial variability of the foliation orientation could be significant to slope design. A robust risk management plan to mitigate this major risk must be successfully implemented in order to continue mining safely by achieving optimal slope.

10 ACKNOWLEDGEMENT

The authors thank ArcelorMittal Mining Canada for their support of this project.

11 REFERENCES

Golder 2019. Geophysical surveys. Internal technical report. Dated November 2019.

GroundProbe 2020. Geotechnical support services: GSS-Remote Monitoring.

Henriquez, F., Kabuya, J.M., Tinucci, J. 2018. Slope Stability Assessment - Z Pit Pushback. Internal technical report. Dated September 2018

Kabuya, J.M. and Henriquez, F. 2017. Phase 1 South East Instability Assessment – Preliminary Results, Internal technical report. Dated December 2017.

Kabuya, J.M., Simon, R., Carvalho, J., Haviland, D. 2020a. Numerical back-analysis of highwall instability in an open pit: a case study. *Proceedings, Slope Stability 2020: International Symposium on Slope Stability in Open Pit Mining and Civil Engineering,* Perth, Australia, pp. 937-952.

Kabuya, J.M., Lambert, J.S., Simon, R. 2020b. Blasting mitigation measures used to control a highwall failure risk, *Proceedings, ISEE 2020: International Society of Explosives Engineers,* Denver, USA, (paper 20v111g).

Maptek 2018. Maptek PerfectDig: powerful design conformance solution, https://www.maptek.com/products/perfectdig/index.html

Noon, D. 2003. Slope Stability Radar for Monitoring Mine Walls, *Mining Risk Management Conference,* Sydney, NSW, pp. 1-12.

Piteau 2016. Geotechnical Slope Stability Analysis and Design for the 2015 Pit Mine Plan. Technical report prepared by Piteau Associates Engineering Ltd. Dated May 2016.

Read, J. and Stacey, P. (eds) 2009. *Guidelines for open pit slope design*. CSIRO Publishing, Australia.

RocWare 2016. WellCAD, https://www.rockware.com/product/wellcad/

Saunders, P., Kabuya, J.M., Torres, A., Simon, R. 2020. Post-blast slope stability monitoring with slope stability radar. *Proceedings, Slope Stability 2020: International Symposium on Slope Stability in Open Pit Mining and Civil Engineering,* Perth, Australia, pp. 507-522.